Progress In Electromagnetics Research, Vol. 159, 49–57, 2017

On the Radiation from a Short Current-Carrying Straight Wire Oriented Perpendicular to a Stratified Medium

Mauro Parise[1, *] and Giulio Antonini[2]

Abstract—In a previous work, improved full-wave analytical expressions have been derived for the Sommerfeld Integrals (SIs) describing electromagnetic radiation from a short vertical straight wire located in close proximity to a conductive soil. Such formulas ensure high accuracy of the result of the computation, as well as time savings with respect to conventional techniques used to evaluate the SIs, but unfortunately may be used only when both source and field points are located at the air-medium interface. The scope of this paper is to overcome the limitations implied by the previous approach, and provide series-form expressions for the generated field components that are valid for an arbitrarily stratified medium and for any position of the vertical wire antenna and observation point in the air space above it. The expressions follow from the analytical evaluation of the integral representation for the magnetic vector potential, performed through contour integration after substituting an equivalent pole set for each branch cut of the integrand. Validity, efficiency and accuracy of the developed formulas are illustrated through numerical examples.

1. INTRODUCTION

The study of the radiation characteristics of dipole antennas situated in proximity to stratified media has attracted the interest of several scientists in the past years [1–20]. This is because electric dipoles are extensively used in a variety of engineering applications, especially in the areas of close-to-the-surface radio communication, geophysical prospecting, radio remote sensing, and hypethermia [2–7, 11–15, 22, 23]. Despite the number of contributions from researchers, to date accurate analytical expressions for the fields, valid regardless of the operating frequency, can be derived only under the assumption that both the source and the observation points lie on the surface of the material medium [10, 23]. If this condition cannot be met, closed-form expressions for the fields may still be obtained, but at the price of introducing approximations that limit their applicability to electrically dense media [4–7, 11] or specified frequency ranges [4–6, 17–20]. Examples of contributions in this direction are the solutions valid for the quasi-static, indermediate, and far-field frequency ranges, which result from reducing the Sommerfeld integrals to forms amenable to asymptotic techniques such as the saddle-point method [13, 17–20].

The present paper focuses on the problem of a short current-carrying straight wire oriented perpendicular to a stratified ground. The scope of the work is to overcome the limitations implied by the approach described in [10, 23], and determine exact analytical expressions for the generated fields that are valid for any position of the source and observation points in the air space above the medium. To accomplish this task, first the direct field and the ideal reflected field are extracted from the integral representation for the magnetic vector potential. Next, the remaining part of the magnetic vector potential is written as the sum of branch-cut integrals and closed-contour integrals around the poles of the integrand. Finally, the hyperbolic branch cuts are extracted from the integrands of the

Received 9 April 2017, Accepted 2 June 2017, Scheduled 30 June 2017

* Corresponding author: Mauro Parise (m.parise@unicampus.it).

[1] Unit of Electrical Engineering, University Campus Bio-Medico of Rome, Italy. [2] Department of Industrial Engineering, Computer Science and Economics, University of L'Aquila, Italy.

branch-cut integrals and replaced with equivalent pole sets [23], so as to make it possible analytical integration. Each field component is given as the sum of two exponential terms (describing the direct and the ideal reflected fields) and three fast convergent sequences of residue sums, that represent the above surface ground wave, the lateral wave and the surface waves. The obtained formulas for the fields offer advantages in terms of time savings with respect to standard numerical integration procedures. Moreover, investigating the expressions for the different contributions to the fields, as well as their outcomes, allows to gain useful insight into the physics of the problem, and this feature makes the proposed solution advantageous over numerical simulation tools employed to solve electromagnetic boundary value problems.

2. FORMULATION OF THE PROBLEM

The geometrical configuration under study is sketched in Fig. 1. The emitter, modeled as a vertical electric dipole of moment $1 \cdot e^{j\omega t}\,\mathrm{A}\cdot\mathrm{m}$, is located at height h above an N-layer conducting medium. The nth layer of the medium has dielectric permittivity ϵ_n, electrical conductivity σ_n, and thickness $d_n{=}z_n - z_{n-1}$, being z_n the position of the upper bound of the layer. The bottom or first layer is assumed to be a semi-infinite region. The magnetic permeability is everywhere equal to that of free space μ_0. We introduce a cylindrical coordinate system (ρ, φ, z) such that the air-medium interface coincides with the plane $z{=}0$ and the short wire antenna is placed on the z axis. The symmetry about the z axis implies that the electromagnetic field originates from a z-directed magnetic vector potential [17]. As a consequence, the field components produced in the air space may be expressed as

$$E_\rho = -\frac{j\omega}{k_0^2}\frac{\partial^2 A}{\partial\rho\partial z}, \tag{1}$$

$$E_z = \frac{j\omega}{k_0^2}\left(\frac{\partial^2}{\partial\rho^2} + \frac{1}{\rho}\frac{\partial}{\partial\rho}\right)A, \tag{2}$$

$$H_\varphi = -\frac{1}{\mu_0}\frac{\partial A}{\partial\rho}, \tag{3}$$

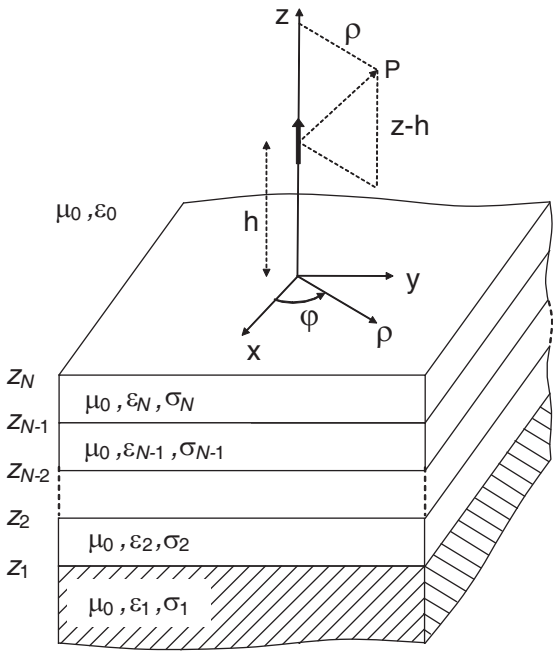

Figure 1. Sketch of a short straight wire oriented perpendicular to a stratified medium.

where A is the non-null component of the vector potential, given by

$$A(\rho,z,h)=\frac{\mu_0}{4\pi}\left[\frac{e^{-jk_0R}}{R}-\frac{e^{-jk_0R'}}{R'}\right]+A^s(\rho,z,h), \tag{4}$$

being

$$A^s(\rho,z,h)=\frac{\mu_0}{4\pi}\int_{-\infty}^{\infty}e^{-u_0(z+h)}\frac{Z_0}{Z_0+\hat{Z}_N}\frac{\lambda}{u_0}H_0^{(1)}(\lambda\rho)d\lambda \tag{5}$$

and

$$R=\sqrt{\rho^2+(z-h)^2}, \qquad R'=\sqrt{\rho^2+(z+h)^2}, \tag{6}$$

$$u_n=\sqrt{\lambda^2-k_n^2}, \qquad \mathrm{Re}[u_n]>0, \tag{7}$$

$$k_n^2=\omega^2\mu_n\epsilon_n-j\omega\mu_n\sigma_n. \tag{8}$$

In Eq. (4), the two exponential terms represent the primary field and the ideal field reflected by the medium (that is the field of a negative image), while A^s is a correction term caused by the imperfect conductivity of the layered half-space. On the other hand, Z_n is the intrinsic impedance of the nth layer (n=0 denotes free space), given by

$$Z_n=\frac{u_n}{\sigma_n+j\omega\epsilon_n}, \tag{9}$$

while $\hat{Z}_n$ is the surface impedance at z=z_n, defined by the recursive formula

$$\hat{Z}_n=Z_n\frac{\hat{Z}_{n-1}+Z_n\tanh(u_nd_n)}{Z_n+\hat{Z}_{n-1}\tanh(u_nd_n)}, \qquad n=2,\ldots,N, \tag{10}$$

with

$$\hat{Z}_1=Z_1. \tag{11}$$

The aim of this paper is to analytically evaluate Eq. (5) and, subsequently, the field components in Eqs. (1)–(3). To this end, it is first convenient to rewrite Eq. (5) as

$$A^s(\rho,z,h)=\frac{\mu_0}{4\pi}\int_{-\infty}^{\infty}G(u_0,u_1,\lambda,z,h)\,H_0^{(1)}(\lambda\rho)\lambda d\lambda, \tag{12}$$

with

$$G(u_0,u_1,\lambda,z,h)=\frac{e^{-u_0(z+h)}}{u_0}\frac{Z_0}{Z_0+\hat{Z}_N}, \tag{13}$$

where the dependence on the square roots $u_2,u_3,\ldots,u_N$ has not been made explicit to signify that the function G is even in such quantities [17]. Next, proceeding as in [17, 24] makes it possible to deform the integration contour so that it is wrapped around the singularities of the integrand located in the upper-half of the complex plane, as shown in Fig. 2(a). This leads to express A^s as

$$A^s(\rho,z,h)=\sum_m\oint_{\lambda_m^{(-1)}}[\ldots]+\int_{-k_0}[\ldots]+\int_{-k_1}[\ldots]=I^{(-1)}+I^{(0)}+I^{(1)}, \tag{14}$$

that is as the sum of two branch-cut integrals associated with $-k_0$ and $-k_1$ plus a number of closed-contour integrals around the poles of G, that is $\lambda_1^{(-1)},\lambda_2^{(-1)},\lambda_3^{(-1)},\ldots$. Notice that the integral along the upper infinite semi-circle has been neglected in Eq. (14). In fact, this contribution cannot but be identically zero, because the Hankel function in the integrand decays exponentially with increasing $|\lambda|$ in the upper half-plane. The explicit form of $I^{(-1)}$ may be easily obtained through residue calculus. It yields

$$I^{(-1)}=\frac{j\mu_0}{2}\sum_m A_m^{(-1)}(z,h)\,H_0^{(1)}\left[\lambda_m^{(-1)}\rho\right], \tag{15}$$

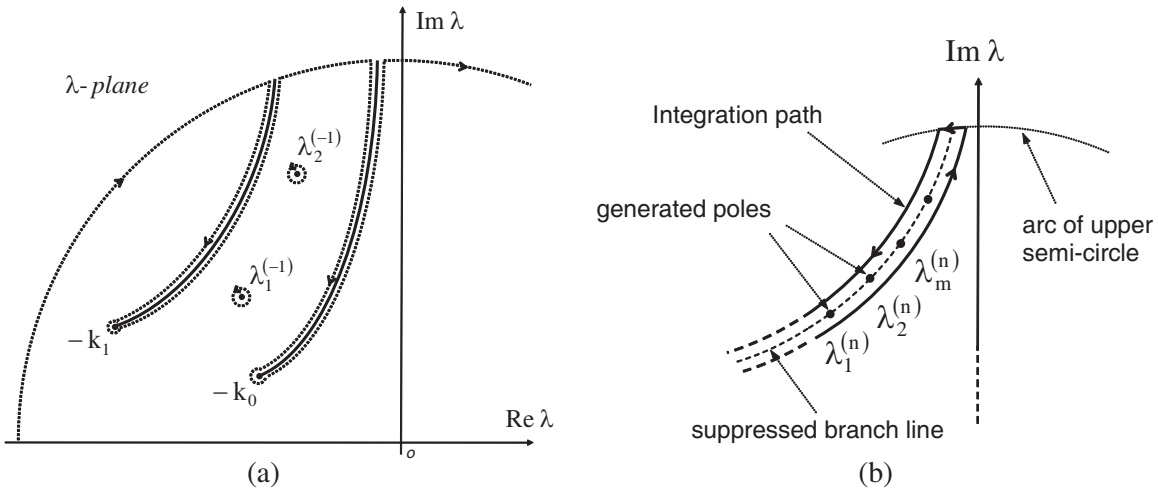

Figure 2. (a) Deformed integration contour and (b) branch cut equivalent pole set.

where $A_m^{(-1)}$ is the residue of the function λG at $\lambda{=}\lambda_m^{(-1)}$, that is

$$A_m^{(-1)}(z,h) = \Re_{\lambda_m^{(-1)}}\left[\lambda\, G(u_0,u_1,\lambda,z,h)\right] = \lim_{\lambda\to\lambda_m^{(-1)}}\left[\lambda{-}\lambda_m^{(-1)}\right]\lambda\, G(u_0,u_1,\lambda,z,h)\,. \tag{16}$$

On the other hand, each of the integrals $I^{(0)}$ and $I^{(1)}$ may be evaluated by extracting the relevant branch cut from the integrand and replacing it with an equivalent set of poles. Branch-cut extraction procedure consists of decomposing G into its even and odd parts with respect to u_0 or u_1. For instance, $I^{(0)}$ requires a decomposition of G with respect to u_0, as follows

$$G(u_0,u_1,\lambda,z,h) = G_e^{(0)}(\lambda,z,h) + G_o^{(0)}(\lambda,z,h)\,u_0, \tag{17}$$

where $G_e^{(0)}$ and $G_o^{(0)}$ are even function of u_0, given by

$$G_e^{(0)}(\lambda,z,h) = \frac{1}{2}\left[G(u_0,u_1,\lambda,z,h) + G(-u_0,u_1,\lambda,z,h)\right], \tag{18}$$

$$G_o^{(0)}(\lambda,z,h) = \frac{1}{2u_0}\left[G(u_0,u_1,\lambda,z,h) - G(-u_0,u_1,\lambda,z,h)\right]. \tag{19}$$

Since $G_e^{(0)}$ does not exhibit any branch cut running from $-k_0$, it will not contribute to $I^{(0)}$. As a consequence, it yields

$$I^{(0)} = \frac{\mu_0}{4\pi}\int_{-k_0} G_o^{(0)}(\lambda,z,h)\,u_0 H_0^{(1)}(\lambda\rho)\lambda d\lambda, \tag{20}$$

and, analogously, for I_1 one obtains

$$I^{(1)} = \frac{\mu_0}{4\pi}\int_{-k_1} G_o^{(1)}(\lambda,z,h)\,u_1 H_0^{(1)}(\lambda\rho)\lambda d\lambda, \tag{21}$$

with

$$G_o^{(1)}(\lambda,z,h) = \frac{1}{2u_1}\left[G(u_0,u_1,\lambda,z,h) - G(u_0,-u_1,\lambda,z,h)\right]. \tag{22}$$

Pole sets equivalent to the extracted branch cuts may be determined by iteratively applying the square root algorithm to the computation of the square roots u_0 and u_1, as described in [10, 23, 24]. At the lth iteration, the square root algorithm generates the following partial-fraction representation for u_n [23]

$$u_n \cong 2^{-l}\left(u_n^2 + \sum_{h=0}^{l-1} 2^{2h}\right) + \sum_{m=1}^{M_l}\frac{r_{mn}}{\lambda_m^{(n)}}\left[\frac{1}{\lambda-\lambda_m^{(n)}} - \frac{1}{\lambda+\lambda_m^{(n)}}\right], \tag{23}$$

being $M_l{=}2^{l-1}-1$, and

$$\lambda_m^{(n)} = -\sqrt{k_n^2 - t_m^2}, \tag{24}$$

$$r_{mn} = \frac{1}{2^{l+1}} \sum_{h=0}^{M_l+1} \binom{2^l}{2h} \left[-t_m^2\right]^h \prod_{\substack{h=1 \\ h\neq m}}^{M_l} \left[t_h^2 - t_m^2\right]^{-1}, \tag{25}$$

with

$$t_m{=}\tan\left(\frac{m\pi}{2^l}\right). \tag{26}$$

Substituting Eq. (23) in the nth branch-cut integral $I^{(n)}$ and closing the integration contour with the arc of upper infinite semi-circle comprised between its ends, as sketched in Fig. 2(b), allows to obtain a closed-contour integral around the $\lambda_m^{(n)}$'s. In fact, such poles lie on the suppressed branch line. Since the residue of Eq. (23) at $\lambda{=}\lambda_m^{(n)}$ is equal to

$$\lim_{\lambda\to\lambda_m^{(n)}} \left[\lambda{-}\lambda_m^{(n)}\right] u_n{=}\frac{r_{mn}}{\lambda_m^{(n)}}, \qquad n=0,1, \tag{27}$$

one obtains

$$I^{(n)} = \frac{j\mu_0}{2} \sum_{m=1}^{M_l} r_{mn} \left[G_o^{(n)}\left(\lambda, z, h\right) H_0^{(1)}(\lambda\rho)\right]_{\lambda=\lambda_m^{(n)}}, \qquad n=0,1, \tag{28}$$

and, after letting $A_m^{(n)}\left(z,h\right){=}r_{mn}\, G_o^{(n)}\left[\lambda_m^{(n)}, z, h\right]$, with $n{=}0,1$, expression (14) for A^s may be rewritten in compact form as

$$A^s\left(\rho,z,h\right){=}\frac{j\mu_0}{2} \sum_{n=-1}^{1} \sum_{m=1}^{M_l} A_m^{(n)}\left(z,h\right) H_0^{(1)}\left[\lambda_m^{(n)}\rho\right], \tag{29}$$

where the first M_l poles of the pole set corresponding to $n{=}-1$ have been considered. It is understood that the numbering of the $\lambda_m^{(-1)}$'s is arranged so that $\mathrm{Im}\,\lambda_1^{(-1)}{<}\,\mathrm{Im}\,\lambda_2^{(-1)}{<}\,\mathrm{Im}\,\lambda_3^{(-1)}{<}\ldots$ and so on, which means that higher-order poles correspond to highly attenuated waves. Finally, use of Eqs. (4) and (29) in Eqs. (1)–(3) gives rise to the following expressions for the fields

$$E_\rho = E_{\rho 0}|_{\zeta=z-h} - E_{\rho 0}|_{\zeta=z+h} + E_\rho^s, \tag{30}$$

$$E_z = E_{z0}|_{\zeta=z-h} - E_{z0}|_{\zeta=z+h} + E_z^s, \tag{31}$$

$$H_\varphi = H_{\varphi 0}|_{\zeta=z-h} - H_{\varphi 0}|_{\zeta=z+h} + H_\varphi^s, \tag{32}$$

being

$$E_{\rho 0} = \frac{\rho\,\zeta e^{-jk_0 r}}{4\pi j\omega\epsilon_0 r^5}\left(3+3jk_0 r - k_0^2 r^2\right), \tag{33}$$

$$E_{z0} = \frac{e^{-jk_0 r}}{4\pi j\omega\epsilon_0 r^5}\left[\left(2\zeta^2-\rho^2\right)\left(1+jk_0 r\right)+\rho^2 k_0^2 r^2\right], \tag{34}$$

$$H_{\varphi 0} = \frac{\rho e^{-jk_0 r}}{4\pi r^3}\left(1+jk_0 r\right), \tag{35}$$

with $r{=}\sqrt{\rho^2{+}\zeta^2}$, and

$$E_\rho^s = -\frac{1}{2\omega\epsilon_0} \sum_{n=-1}^{1} \sum_{m=1}^{M_l} \lambda_m^{(n)} \frac{dA_m^{(n)}}{dz} H_1^{(1)}\left[\lambda_m^{(n)}\rho\right], \tag{36}$$

$$E_z^s = \frac{1}{2\omega\epsilon_0} \sum_{n=-1}^{1} \sum_{m=1}^{M_l} \left[\lambda_m^{(n)}\right]^2 A_m^{(n)} H_0^{(1)}\left[\lambda_m^{(n)}\rho\right], \tag{37}$$

$$H_\varphi^s = \frac{j}{2} \sum_{n=-1}^{1} \sum_{m=1}^{M_l} \lambda_m^{(n)} A_m^{(n)} H_1^{(1)}\left[\lambda_m^{(n)}\rho\right], \tag{38}$$

with

$$\frac{dA_m^{(n)}}{dz}=\begin{cases}\Re_{\lambda_m^{(-1)}}\left[-u_0\,\lambda\,G\left(u_0,u_1,\lambda,z\right)\right], & n=-1\\ -r_{mn}\,G_e^{(0)}\left[\lambda_m^{(0)},z\right], & n=0\\ -r_{mn}\,u_0\,G_o^{(1)}\left[\lambda_m^{(1)},z\right], & n=1\end{cases} \tag{39}$$

where account has been taken of the identities [21]

$$\frac{dH_0^{(1)}\left(\lambda\rho\right)}{d\rho} = -\lambda H_1^{(1)}\left(\lambda\rho\right), \tag{40}$$

$$\left(\frac{\partial^2}{\partial\rho^2}+\frac{1}{\rho}\frac{\partial}{\partial\rho}\right)H_0^{(1)}\left(\lambda\rho\right) = -\lambda^2 H_0^{(1)}\left(\lambda\rho\right). \tag{41}$$

Each of the expressions (36)–(38) consists of three sequences of residue sums, which converge as l is increased in virtue of convergence of the square root algorithm. The residue sums associated with n=0 and n=1 describe the above-surface ground and lateral waves, respectively. Such contributions, together with the direct field and the ideal reflected field, labelled with a subscript 0 in Eqs. (30)–(32), constitute the space wave radiated by the antenna. The rest of the generated field consists of surface waves, and is described by the residue sums associated with $n=-1$ in Eqs. (36)–(38). Expressions (30)–(32) allow to overcome the limitations implied by the previously published square-root-algorithm-based solution to the same problem [10, 24]. In fact, they allow to relax the assumption that both source and observation points lie at the air-medium interface. At the same time, as will be clarified in Sec. 3, the derived expressions ensure a high level of accuracy and offer advantages in terms of time savings with respect to standard numerical techniques conventionally used for evaluating Sommerfeld-type integrals.

3. RESULTS AND DISCUSSION

Primary objective of this section is to show the convergence of the sequences in Eqs. (36)–(38) as the number of iterations l of the square root algorithm is increased. To this goal, we use Eq. (31) to compute the amplitude-frequency spectrum of the E_z-field generated by a unit-moment straight wire antenna lying on the top surface of a two-layer conductive ground. The field point is at height z=50 m above the medium and at radial distance ρ=300 m from the emitter, while the electromagnetic and geometric parameters of the layers of the medium are assumed to be σ_1=10 mS/m, ϵ_1=10ϵ_0, d_1=400 m, σ_2=1 S/m, and ϵ_2=5ϵ_0. The results of the simulations, depicted in Fig. 3, are compared with the data arising from numerically evaluating Eq. (2) through the Gauss-Kronrod quadrature rule [25]. As is seen, when l is increased the outcomes from Eq. (31) rapidly converge to the exact numerical data, denoted by points, and convergence is faster at higher frequencies. Moreover, perfect agreement between analytical and numerical data is observed when truncating the sequences of residue sums in Eq. (37) at l=12, that is when each residue sum is composed of $M_{12}=2^{11}-1=2047$ residues. It should be noted that, in general, the three contributions to Eq. (37) do not have the same impact on the E_z-field strength. For instance, if the field point is located at height z=50 m from the top surface of the medium, one would expect that the effects of surface and lateral waves, associated with n=−1 and n=1, respectively, are negligible with respect to that of the ground wave (n=0). This point is clarified by Fig. 4, which depicts the magnitude of E_z and those of the relevant ground-wave, lateral-wave, and surface-wave terms against the radial distance ρ from the emitter. The parameters of the medium are taken to be the same as in the previous example, and the operating frequency is assumed to be 10 kHz. Again, the sequences of the residue sums have been truncated at l=12. From the analysis of the plotted curves it emerges that the amplitude of the E_z-field substantially coincides with that of the ground-wave field over the considered interval, and that the surface waves suffer from a mild attenuation with increasing ρ. Instead, the magnitude of the lateral wave rapidly goes down below the plot scale as ρ grows up. Finally, it should be observed that direct and ideal reflected fields cannot contribute to the total E_z-field, since they cancel out each other because of the position of the emitter at the air-medium interface.

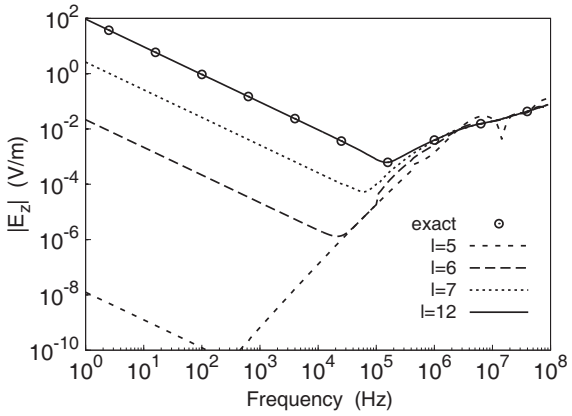

Figure 3. Profiles of $|E_z|$ against frequency. Outcomes from the proposed solution are compared with the data arising from numerical integration of the field integral.

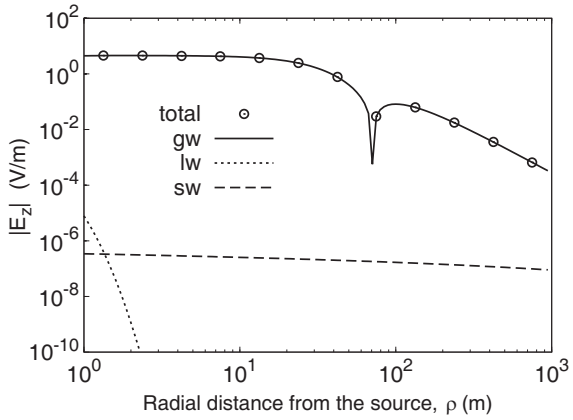

Figure 4. Profile of $|E_\rho|$ against ρ. Separate contributions of ground wave (gw), lateral wave (lw), and surface waves (sw) to the total field.

One would ask whether the derived solution is advantageous in terms of computation time over previous solutions and standard numerical integration procedures. This aspect is illustrated in Table 1, which shows the time taken by the proposed method, the Gauss-Kronrod quadrature rule, and King's well-established solution [7], to calculate the radial distribution of the vertical electric field that a straight wire antenna lying on a homogeneous medium produces at z=50 m. Here, the operating frequency is 1 MHz, while the electromagnetic parameters of the medium are taken to be σ_1=0.1 mS/m and ϵ_1=3 ϵ_0.

Table 1 is structured as follows. The second column contains time cost data corresponding to

Table 1. Computation times and accuracy of the proposed and conventional approaches.

Approach	Time consumption (s)	Speed-up	RMS rel. error (%)
Gaussian rule	126	21	-
King's approach	6	-	8.3
Proposed solution	19	3.2	0.16

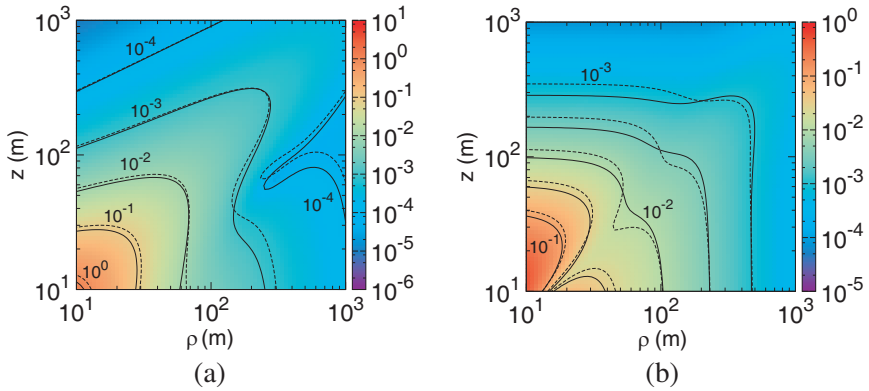

Figure 5. Contour plots of (a) $|E_\rho|$ and (b) $|E_z|$ versus ρ and z, computed for σ_1=0.1 mS/m and ϵ_1=3 ϵ_0 by applying the proposed approach (solid isolines). Outcomes from King's approach are denoted by dashed isolines.

simulations running on a single-core 1.8 GHz PC. The third column shows the ratio of the time taken by the proposed expression for E_z and the Gaussian rule to that required by King's solution (speed-up offered by King's approach). Finally, the fourth column contains the root-mean-square (RMS) relative errors resulting from using the proposed and King's solution in place of Gaussian quadrature rule. From a glance at the data in Table 1 it is deduced that, accuracy being equal, using Eq. (37) rather than Gaussian quadrature permits to obtain significant time savings. On the other hand, King's approach implies minimum time cost, but the price to be paid for its usage is the loss of accuracy. This is also confirmed by the contour plots sketched in Fig. 5, which depict the magnitudes of E_ρ (Fig. 5(a)) and E_z (Fig. 5(b)) versus ρ and z (the antenna is still positioned at height h=0). For both the contour plots, a significant discrepancy is observed between the solid isolines associated with the proposed solution and the dashed isolines arising from King's approach. The amount of the discrepancy depends on the conductivity of the medium, and higher values of the conductivity make it possible to reduce the discrepancy. For instance, assuming σ_1=1 mS/m and ϵ_1=10 ϵ_0 leads to the contour plots illustrated in Fig. 6, characterized by solid and dashed isolines almost overlapping. Bad accuracy of King's solution for low values of the conductivity is explained by the failure of the assumptions $|k_1|\rho \gg 1$ and $k_0^2/|k_1^2| \ll 1$, underlying its derivation.

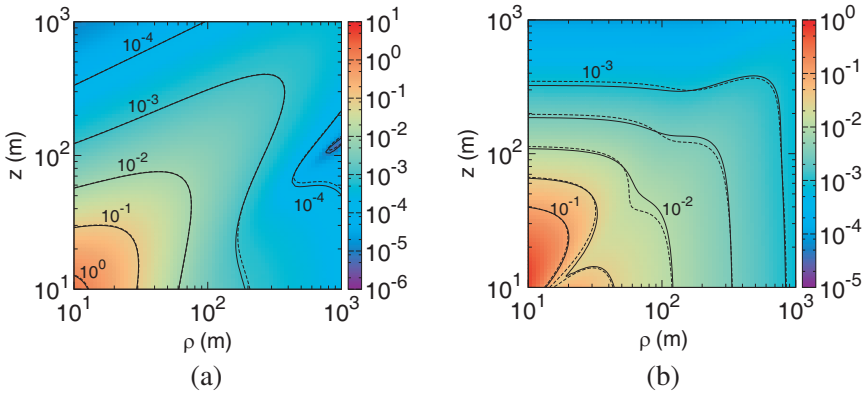

Figure 6. Contour plots of (a) $|E_\rho|$ and (b) $|E_z|$ versus ρ and z, computed for σ_1=1 mS/m and ϵ_1=10 ϵ_0 by applying the proposed approach (solid isolines). Outcomes from King's approach are denoted by dashed isolines.

4. CONCLUSION

This paper presents an explicit solution, in series form, for the fields from a short current-carrying straight wire oriented perpendicular to a stratified medium. The solution arises from the analytical evaluation of the integral representation for the magnetic vector potential, carried out through contour integration upon substituting an equivalent pole set for each branch cut exhibited by the integrand. Each field component is expressed as the sum of five contributions, namely the direct, the ideal reflected, the ground-wave, the lateral-wave, and the surface-wave fields. The latter three terms are given as convergent sequences of residue sums. Performed numerical simulations confirm the correctness of the developed theory. It has been shown how the proposed formulas are accurate and significantly less time consuming than conventional numerical integration procedures.

REFERENCES

1. Sommerfeld, A., "On the propagation of waves in wireless telegraphy," *Annals of Physics*, Vol. 81, 1135–1153, 1926.
2. Baños, A., *Dipole Radiation in the Presence of a Conducting Half-space*, Pergamon Press, Oxford, NY, 1966.

3. Durrani, S. H., "Air to undersea communication with electric dipoles," *IRE Transactions on Antennas and Propagation*, Vol. 10, 524–528, 1962.
4. Moore, R. K. and W. E. Blair, "Dipole radiation in a conducting half space," *Journal of Research of the National Bureau of Standards-D Radio Propagation*, Vol. 65D, No. 6, 547–563, 1961.
5. Wait, J. R., "The electromagnetic fields of a horizontal dipole in the presence of a conducting half-space," *Canadian Journal of Physics*, Vol. 39, 1017–1028, 1961.
6. Bannister, P. R., "Quasi-static fields of dipole antennas at the earth's surface," *Radio Science*, Vol. 1, 1321–1330, 1966.
7. King, R. W. P., M. Owens, and T. T. Wu, *Lateral Electromagnetic Waves: Theory and Applications to Communications, Geophysical Exploration, and Remote Sensing*, Springer-Verlag, New York, 1992.
8. King, R. W. P., S. S. Sandler, and L. C. Shen, "The electromagnetic field of a vertical electric dipole over the earth or sea," *IEEE Transactions on Antennas and Propagation*, Vol. 42, 382–389, 1994.
9. King, R. W. P., "Electromagnetic field of a vertical dipole over an imperfectly conducting half-space," *Radio Science*, Vol. 25, 149–160, 1990.
10. Parise, M., "An exact series representation for the EM field from a vertical electric dipole on an imperfectly conducting half-space," *Journal of Electromagnetic Waves and Applications*, Vol. 28, No. 8, 932–942, 2014.
11. Wait, J. R., *Electromagnetic Waves in Stratified Media*, Pergamon Press, New York, 1970.
12. Parise, M., "Second-order formulation for the quasi-static field from a vertical electric dipole on a lossy half-space," *Progress In Electromagnetics Research*, Vol. 136, 509–521, 2013.
13. Kong, J. A., *Electromagnetic Wave Theory*, John Wiley & Sons, New York, 1986.
14. Ward, S. H. and G. W. Hohmann, "Electromagnetic theory for geophysical applications," *Electromagnetic Methods in Applied Geophysics*, Vol. 1, 130–311, Society of Exploration Geophysicists, Tulsa, OK, 1988.
15. Balanis, C. A., *Antenna Theory: Analysis and Design*, 2nd Edition, John Wiley & Sons, New York, 1997.
16. Wait, J. R., "Radiation from a vertical electric dipole over a stratified ground," *Transactions of the IRE — Antennas and Propagation*, Vol. 1, No. 1, 9–11, 1953.
17. Wait, J. R., "Influence of a sub-surface insulating layer on electromagnetic ground wave propagation," *IEEE Transactions on Antennas and Propagation*, Vol. 14, No. 6, 755–767, 1966.
18. Wait, J. R., "Asymptotic theory for dipole radiation in the presence of a lossy slab lying on a conducting half-space," *IEEE Transactions on Antennas and Propagation*, Vol. 15, No. 5, 645–648, 1967.
19. Kong, J. A., L. C. Shen, and L. Tsang, "Field of an antenna submerged in a dissipative dielectric medium," *IEEE Transactions on Antennas and Propagation*, Vol. 25, No. 6, 887–889, 1977.
20. Fuller, J. A. and J. R. Wait, "A pulsed dipole in the earth," *Transient Electromagnetic Fields*, 237–269, Springer, New York, 1976.
21. Parise, M., "An exact series representation for the EM field from a circular loop antenna on a lossy half-space," *IEEE Antennas and Wireless Prop. Letters*, Vol. 13, 23–26, 2014.
22. Parise, M., "Exact EM field excited by a short horizontal wire antenna lying on a conducting soil," *AEU-International Journal of Electronics and Communications*, Vol. 70, 676–680, 2016.
23. Parise, M., "Improved Babylonian square root algorithm-based analytical expressions for the surface-to-surface solution to the Sommerfeld half-space problem," *IEEE Transactions on Antennas and Propagation*, Vol. 63, No. 12, 5832–5837, 2015.
24. Parise, M., "On the surface fields of a small circular loop antenna placed on plane stratified earth," *International Journal of Antennas and Propagation*, Vol. 2015, 1–8, 2015.
25. Patterson, T. N. L., "The optimum addition of points to quadrature formulae," *Mathematics of Computation*, Vol. 22, 847–856, 1968.